Stochastic Geometry Design for Cell-Free Coded Random Access

Lorenzo Valentini, *Member, IEEE*, Marco Chiani, *Fellow, IEEE*, and Enrico Paolini, *Senior Member, IEEE*

***Abstract*— Grant-free access schemes, capable to reduce control signaling and device complexity, are good candidates to support future massive multiple access applications. In the same direction, cell-free architectures promise to pave the way to fairness in power consumption and performance among the users. The combination of these two ingredients has the potential to interconnect a large number of low-power devices to the network. In this letter, a theoretical analysis tool for grant-free coded random access, based on stochastic geometry and density evolution, is developed in the context of cell-free architectures. In sharp contrast with the cell-based scenario, we found out that temporally repeating less packets is a valid option due to the exploitation of spatial repetitions given by the cell-free topology.**

***Index Terms*— Cell-free massive MIMO, coded random access, density evolution, grant-free access, stochastic geometry.**

I. Introduction

RECENTLY, cell-free network architectures have been introduced in response to the challenges posed by inter-cell interference in the context of the increasing network densification and to the need of a higher user fairness in terms of energy and performance [1], [2]. The appellative "cell-free" refers to networks that comprise a large number of geographically distributed access points (APs), connected to processors which coordinate their activities through fronthaul links. This new architectural approach shows great potential for low-power devices by improving coverage and reducing communication distances, allowing devices to operate with lower power [2].

Stochastic geometry has proven effective in establishing a mathematical framework for modeling diverse multi-user wireless communication scenarios and assessing their performance [3]. For example, sticking to its applications to cell-free networks, the occurrence of channel hardening and favorable propagation phenomena was investigated in [4]. Moreover, both downlink achievable rate and coverage probability were addressed in [5], considering a random placement of the APs. Imposing a finite fronthaul capacity, the system energy efficiency was analyzed in [6], varying the number of antennas per AP. Another example is represented by [7], where the blockage of mmWave fronthaul links between APs and central processing units was evaluated through stochastic geometry. In this context, our work addresses the medium access control (MAC) layer analysis of grant-free uplink protocols. In particular, we target coded random access (CRA) schemes, where coding is used together with successive interference cancellation (SIC) [8].

Density evolution is a fundamental tool for analysis and design of modern channel codes with iterative decoding [9]. It was applied in [8] to design CRA schemes, in particular to optimize irregular repetition slotted ALOHA (IRSA) over the collision channel. This approach was extended to coded slotted ALOHA (CSA) in [10]. The assumptions in [8] and [10] can be summarized as: i) if multiple transmissions occur simultaneously, then the receiver is unable to successfully decode any of the messages; ii) if there is only one transmission, then the corresponding message is decoded with zero error probability; iii) decoded messages and their replicas in other slots are perfectly subtracted. These assumptions, usually referred to as collision channel assumptions, permit to efficiently carry out performance analysis and optimization of CRA schemes. This optimization is often performed with respect to the traffic load using evolutionary algorithms [11], [12], [13]. In other works, optimization is carried out targeting different goals, such as the total power consumption [14].

In this letter, we interconnect the three topics above by developing a novel theoretical analysis, based on density evolution and stochastic geometry, to design CRA schemes in cell-free architectures. The derivation assumes that users and APs follow homogeneous Poisson point processes (PPPs). Each AP is able to receive user packets transmitted in its coverage area, leading to a natural extension of the collision channel assumptions. Since the APs are connected, the redundancy provided by spatial and temporal packet replicas can be exploited by SIC. The proposed analysis can capture both a path-loss only model, where the AP coverage area has the shape of a disk, and a path-loss plus shadowing model. The main contributions of the letter can be summarized as follows: i) we derive stochastic geometry-based density evolution equations for CRA in cell-free architectures; ii) we derive lower bounds to estimate error floors, which are not captured by density evolution analysis; iii) we show that optimal IRSA distributions derived for the cell-based scenario may turn sub-optimum in cell-free architectures, when the AP density increases. Monte Carlo simulation results are shown to prove the effectiveness of the proposed approach.

II. Preliminary and Background

This section briefly reviews density evolution for IRSA over the collision channel [8]. There are K_{a} active users

Manuscript received 17 May 2024; accepted 21 June 2024. Date of publication 27 June 2024; date of current version 14 August 2024. Supported in part by the CNIT/WiLab and the WiLab-Huawei Joint Innovation Center, and in part by the European Union through the Italian National Recovery and Resilience Plan of NextGenerationEU, partnership on "Telecommunications of the Future" under Grant PE00000001- "RESTART." The associate editor coordinating the review of this letter and approving it for publication was P. Cardieri. *(Corresponding author: Enrico Paolini.)*

The authors are with CNIT/WiLab, DEI, University of Bologna, 47522 Cesena, Italy (e-mail: lorenzo.valentini13@unibo.it; marco.chiani@unibo.it; e.paolini@unibo.it).

Digital Object Identifier 10.1109/LCOMM.2024.3420110

that contend to transmit one message each in a frame with N_s slots. Each active user transmits multiple replicas of its packet in the frame, where the packet repetition degree r is a random variable with probability generating function (PGF) $\Lambda(x) = \sum_r \Lambda_r x^r$, drawn independently by each active user. The system is represented by a bipartite graph with K_a user nodes and N_s slot nodes: if a user sends r packet replicas in the frame then its user node has degree r, i.e., r connected edges, towards the r slot nodes associated with its chosen slots. The degree of a slot node, c, is the number of users that have picked the corresponding slot; its PGF is $\Psi(x) = \sum_c \Psi_c x^c$, where Ψ_c is the probability that a slot node has degree c. The probabilities that an edge is connected to a degree-r user node and degree-c slot node are $\lambda_r = \Lambda_r\, r/\Lambda'(1)$ and $\rho_c = \Psi_c\, c/\Psi'(1)$, respectively. We also define the polynomials $\lambda(x) = \sum_r \lambda_r x^{r-1}$ and $\rho(x) = \sum_c \rho_c x^{c-1}$. The system load G is defined as $G = K_a/N_s$ [users/slot].

The single receiver processes the whole frame according to an iterative SIC procedure. Under collision channel assumptions, whenever a packet replica is not interfered, it is successfully decoded; the receiver then cancels the interference of the packet and of its twins from the corresponding slots, possibly yielding new successful decoding attempts; the procedure is repeated until no new messages can be decoded. With perfect interference cancellation and in the asymptotic regime $K_a \to \infty$, $N_s \to \infty$, and constant K_a/N_s, the SIC process can be modeled by a simple recursion referred to as density evolution for IRSA. Let: *i)* $q_\ell^{(r)}$ be the probability that an edge is connected to a degree-r user node not yet decoded at the end of SIC iteration ℓ; *ii)* $p_\ell^{(c)}$ be the probability that an edge is connected to a degree-c slot node where a collision persist at the end of SIC iteration ℓ; *iii)* $q_\ell = \sum_r \lambda_r\, q_\ell^{(r)}$ and $p_\ell = \sum_c \rho_c\, p_\ell^{(c)}$ be the corresponding average probabilities.

It is easy to see that $q_\ell^{(r)} = p_{\ell-1}^{r-1}$ and $p_\ell^{(c)} = 1-(1-q_\ell)^{c-1}$. Averaging over the probabilities λ_r and ρ_c yields the recursion

$$p_\ell = 1 - \rho(1 - \lambda(p_{\ell-1})) \tag{1}$$

with initial value $p_0 = 1$ (no revealed edge at the beginning). Moreover, in the asymptotic regime the polynomial $\rho(x)$ involved in (1) assumes the form $\rho(x) = \exp(G\Lambda'(1)(1-x))$.

The asymptotic packet loss rate (PLR) at SIC iteration ℓ is $Q_\ell = \sum_r \Lambda_r p_\ell^r = \Lambda(p_\ell)$. We can then define the asymptotic load threshold of an IRSA distribution $\Lambda(x)$ as

$$G^\star = \sup\{G > 0 : Q_\ell \to Q_\infty \le Q^\star \text{ as } \ell \to \infty\} \tag{2}$$

where $Q^\star$ a target error probability. This threshold definition allows us to capture also the behaviour of schemes with $r = 1$ (as for $r \ge 2$ it is allowed to simply take $Q^\star = 0$).

The above analysis is inherently cell-based, as it holds for a single receiver. In the following, we extend it to cell-free architectures using density evolution described in this section to model the temporal processes, together with PPPs to model the spatial processes of both users and APs.

III. Stochastic Geometry-Based Design

We consider a slotted and framed grant-free uplink access protocol in a cell-free network architecture. Active users contend adopting the IRSA protocol over a frame composed of N_s slots. Both APs and users are scattered in the area covered by the network. To model their spatial positions we use two homogeneous 2-dimensional PPPs [15] with densities η [APs/m^2] and ξ [users/m^2], respectively. A pictorial representation is provided in Fig. 1, where both the spatial and the temporal processes are illustrated.

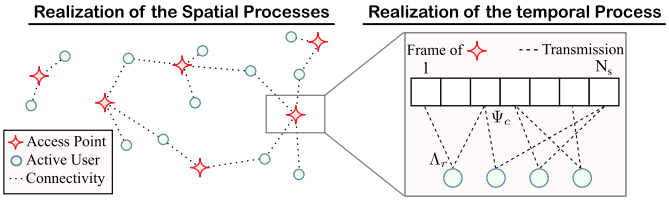

Fig. 1. Example of realizations of the spatial (AP and user positions) and temporal (transmission of replicas in different slots) processes.

We initially model wireless connectivity using a disk model. This simple model naturally arises when considering only the path-loss. Letting α be the path-loss exponent, P_{th} be the receiver sensitivity, P be the power received at a distance of 1 m, and defining $\bar{P}_{th} = P_{th}/P$, we have the following gating effect: receivers at a distance d greater than a radius $R = \bar{P}_{th}^{-1/\alpha}$ are not in wireless connectivity with the transmitter, while receivers inside this radius are connected to it. Furthermore, we assume a collision channel to model the interference effect. Accordingly, APs receiving multiple messages in a slot are not able to decode any of them.

Adopting this disk model over the described scenario with two homogeneous PPPs, unavoidable decoding failures arise due to spatial positions. In fact, if an active user has no APs in connectivity, there is no possibility to decode its message, leading to an error floor in the PLR curve. To avoid this bias, we condition the active users' process to generate users in the coverage area of the APs network, resulting in users having at least one AP in connectivity. Then, the probability that a given user is in connectivity of k different receiving APs is

$$P_\eta(k) = \frac{(\eta\,|\mathcal{A}|)^k}{k!}\,\frac{e^{-\eta\,|\mathcal{A}|}}{1-e^{-\eta\,|\mathcal{A}|}}, \quad k > 0 \tag{3}$$

where the dependence on R is by $|\mathcal{A}| = \pi R^2$. An active user is then connected to $\bar{N}_{AP} = \frac{\eta\,|\mathcal{A}|}{1-e^{-\eta\,|\mathcal{A}|}}$ APs on average. Next, the probability that k active users are connected to a given AP is

$$P_\xi(k) = \frac{(\xi\,|\mathcal{A}|)^k}{k!}\,e^{-\xi\,|\mathcal{A}|}, \quad k \geqslant 0\,. \tag{4}$$

Note that, the generation of the users according to the constraint that each user is in connectivity of at least one AP does not follow anymore a homogeneous PPP. However, for values $\eta\,|\mathcal{A}|$ of interest [4], the process is practically homogeneous.

In presence of log-normal shadowing, two points at distance ζ are in connectivity with each other if $Pe^{2\sigma \mathsf{X}}/\zeta^\alpha > P_{th}$ where $\mathsf{X} \sim \mathcal{N}(0,1)$ and σ is the shadowing parameter [16]. The Gaussian random variable X is modeled as independent from user to user, leading to uncorrelated shadowing effects. A user and an AP at a distance ζ are therefore in connectivity with probability $p(\zeta)$, given by

$$p(\zeta) = \mathbb{P}\left\{P\frac{e^{2\sigma\mathsf{X}}}{\zeta^\alpha} > P_{th}\right\} = \mathcal{Q}\left(\frac{\ln \bar{P}_{th} + \alpha \ln \zeta}{2\sigma}\right) \tag{5}$$

where $\mathcal{Q}(x)$ is the $\mathcal{Q}$-function of the standard normal distribution. For each user (or AP), this selection based on the

received power is independent for each point and gives rise to an independent thinning of the PPP. We can compute an "effective area" of this thinned PPP as [16]

$$|\mathcal{A}| = \int_0^{\infty}\int_0^{2\pi} \zeta p(\zeta) d\theta d\zeta = \pi \exp\left(\frac{8\sigma^2}{\alpha^2} - \frac{2\ln \bar{P}_{\text{th}}}{\alpha}\right). \quad (6)$$

This way, we can analyze in a unified way both the disk model and the shadowing scenario, by incorporating in (3) and (4) the area $|\mathcal{A}| = \pi R^2$ or (6), respectively.

A. Density Evolution for Cell-Free Networks

In the following, we embody the spatial processes described in Section III into the analysis reviewed in Section II by extending (1) from a single receiver (cell-based) scenario to a cell-free one. Hereafter we let $B = \eta|\mathcal{A}|$. From Section II we have that an active user transmits r packet replicas according to the PGF $\Lambda(x)$. Next, in a cell-free setting the user is also in connectivity of k APs, according to (3), leading to a total of $n = r\,k$ repetitions per user. This way, the effective user node degree n is a random variable with PGF

$$\begin{aligned}\Gamma(x) &= \sum_n \Gamma_n x^n = \sum_r \sum_k \Lambda_r P_\eta(k) x^{rk} \\ &= \frac{e^{-B}}{1-e^{-B}} \sum_r \Lambda_r (e^{B\,x^r} - 1) \end{aligned} \quad (7)$$

leading to an equivalent edge-perspective user degree distribution $\gamma(x) = \Gamma'(x)/\Gamma'(1)$. Hence, $\gamma(x)$ plays the role of $\lambda(x)$ in (1) when the cell-free case is considered. Moreover, an AP receives exactly c packets in a slot with probability

$$\begin{aligned}\Psi_c &\overset{(a)}{=} \sum_{k=c}^{\infty} \binom{k}{c} \left(\frac{\Lambda'(1)}{N_s}\right)^c \left(1 - \frac{\Lambda'(1)}{N_s}\right)^{k-c} P_\xi(k) \\ &\overset{(b)}{=} \frac{(\Lambda'(1)\,G)^c}{c!} e^{-\Lambda'(1)\,G} \end{aligned} \quad (8)$$

where: (a) follows from weighting the probability of c out of k users picking the slot, given that the AP has k connected active users, with the probability mass function of k, $P_\xi(k)$; (b) follows from (4) and from re-defining the load as $G = \xi\,|\mathcal{A}|/N_s$ [users/slot]. By $\rho(x) = \sum_c \rho_c x^{c-1}$ and $\rho_c = \Psi_c\, c/\Psi'(1)$, (8) leads to the same formal expression of $\rho(x)$ as in the cell-based case (Section II), $\rho(x) = \exp(G\Lambda'(1)(1-x))$, albeit with a different expression for G.

Replacing the polynomial $\lambda(x)$ in (1) with the edge-perspective user degree distribution $\gamma(x)$ derived from (7), after algebraic manipulation we obtain

$$p_\ell = 1 - \exp\left(-G \sum_r \Lambda_r\, r\, p_{\ell-1}^{r-1} \exp\Big(B\,(p_{\ell-1}^r - 1)\Big)\right) \quad (9)$$

with $p_0 = 1$. The load threshold $G^\star$ of an IRSA distribution $\Lambda(x)$ can thus be computed again by (2), upon re-defining Q_ℓ as $Q_\ell = \Gamma(p_\ell)$. Importantly, if $\Lambda_1 = 0$ (the minimum repetition degree is 2 or larger) then the threshold is well-defined for arbitrarily small $Q^\star$ in (2), since $p_\infty = 0$ (so $Q_\infty = 0$) up to some G. In contrast, if $\Lambda_1 \neq 0$ then a fixed point $p_\infty = 0$ can never be reached for any G, and therefore we need to impose some positive residual error probability $Q^\star > 0$ to have a well-defined threshold. Also note from (9) that, for given $\Lambda(x)$ and considering a disk model, $G^\star$ does not depend on η and R separately, but on $B = \eta\pi R^2$. Moreover, regardless of the connectivity model, each B maps bijectively to an $\bar{N}_{\text{AP}}$ value, so we can think of $G^\star$ as a function of $\bar{N}_{\text{AP}}$.

B. Convergence Analysis for Regular Distributions

In this section we want to elaborate on the analytical study of $G^\star$, assuming a regular distribution $\Lambda(x) = x^r$. In this case we can derive the value of the fixed point $p_\ell = p_{\ell-1} = p$ yielding a target $Q^\star$ as

$$p = \Gamma^{-1}(Q^\star) = \left[\frac{1}{B}\ln\left(1 + Q^\star\left(e^B - 1\right)\right)\right]^{1/r}. \quad (10)$$

Assuming we are free from other constraints, the load threshold from (9) would be

$$G^\star_{\text{free}} = -\ln(1-p)\, e^{B(1-p^r)}/(rp^{r-1}). \quad (11)$$

This load is not achievable if (9) has other fixed points for larger p, which will inevitably stuck the recursion for some $G < G^\star_{\text{free}}$. To see when this happens, we look for the values of p where the function $1 - \rho(1 - \gamma(p))$ (i.e., the right hand side of (9) with $p_{\ell-1} = p$) is tangent to the bisector p. Manipulating (9), we obtain that to have convergence of the iterations starting from $p_0 = 1$ the load cannot be greater than $G^\star_{\text{stuck}}$, defined as the minimum value of $G^\star_{\text{tan}} = \left[e^{B(p^r-1)}\, r(1-p)p^{r-2}\left[r - 1 + Brp^r\right]\right]^{-1}$ such that p is a root of

$$B = h(p) = \frac{(r-1)(1-p)\ln(1-p) - p}{rp^r(1-p)\ln(1-p)}. \quad (12)$$

Summarizing, we have that $G^\star = \min\{G^\star_{\text{free}}, G^\star_{\text{stuck}}\}$, giving rise to a possible phase transition effect.

It is interesting to note that, for the case $r = 1$, we have two roots of $B = h(p)$ represented by $1 + [BW_{0/-1}(-1/B)]^{-1}$ where $W_k(x)$ is the k-th branch of the Lambert W function. This leads to

$$G^\star_{\text{stuck}} = -W_{-1}(-1/B)\exp\left(-1/W_{-1}(-1/B)\right). \quad (13)$$

From the behavior of $W_{-1}(x)$ we also deduce that $G^\star_{\text{stuck}}$ does not exist if $B < e$. For the case $r = 2$, we have that $G^\star_{\text{free}} = e^B/2$ whenever $Q^\star \to 0$ (i.e., $p \to 0$), meaning that we could have phase transition effects. For the cases $r \geq 3$, we have that $G^\star = G^\star_{\text{stuck}}$ for $Q^\star \to 0$, due to the fact that $G^\star_{\text{free}} \to \infty$, meaning that those schemes may not exhibit phase transition effects. These behaviours will be verified in Section IV.

C. Lower Bound Analysis for Disk Model

In this section we derive a lower bound for the PLR assuming disk model connectivity. To derive it, we have to compute the probability that an unresolvable collision occurs. To this aim, we choose the event in which a user and its closest interfering neighbor are in connectivity by exactly the same APs. For interfering user we mean that it is transmitting in the same time slots of the user under examination. For the sake of simplicity, hereafter, we consider $\bar{N}_{\text{AP}}$ sufficiently large to have a homogeneous PPP for user locations.

Let us consider a general IRSA scheme defined by $\Lambda(x)$. Given r replicas, the users have in total $\binom{N_s}{r}$ slot pattern choices for transmission. Therefore, $\Lambda_r \xi / \binom{N_s}{r}$ represents the spatial density of the interfering users. This process is still homogeneous since it arises from a uniform independent thinning of the active users process. Then, considering a generic user, its closest interfering user distance is a random variable δ distributed according to the probability density function

$$f_{\delta}(\delta; r) = \frac{2\pi \Lambda_r \xi \delta}{\binom{N_s}{r}} e^{-\pi \Lambda_r \xi \delta^2 / \binom{N_s}{r}} \qquad \delta \geqslant 0\,. \tag{14}$$

On the other hand, given δ, the probability to share the same APs under the disk model assumption (no shadowing), is the probability that at least one AP resides in the intersection of the two disks $\mathcal{A}_{\text{int}}$ with centers the two users, and no APs reside in the non-overlapping region. The constraint that at least one AP is in $\mathcal{A}_{\text{int}}$ derives from the hypothesis that all users are in connectivity of at least one AP. Solving the geometric problem we have that the intersection area is

$$|\mathcal{A}_{\text{int}}| = 2\ R^2 \arccos\left(\frac{\delta}{2R}\right) - \delta \sqrt{R^2 - \frac{\delta^2}{4}} \tag{15}$$

for $\delta \leq 2R$ and zero otherwise. Finally, the probability of the described collision event, given r, is

$$P(r) = \int_0^{\infty} e^{-\eta(2\pi R^2 - 2|\mathcal{A}_{\text{int}}|)} \left(1 - e^{-\eta |\mathcal{A}_{\text{int}}|}\right) f_{\delta}(\delta; r)\, d\delta \tag{16}$$

and the lower bound on the PLR is $P_{\text{L}} \geq \sum_r \Lambda_r P(r)$.

IV. Numerical Results

As main numerical outcomes: i) we show the dependency of the asymptotic load threshold on the average number of APs in connectivity; ii) we assess the consistency between the proposed analysis tools and Monte Carlo simulations.

A. Density Evolution Analysis

To perform density evolution analysis, we designate a value of G as achievable (i.e., $G < G^{\star}$) when the density evolution recursion yields $Q_{\infty} < Q^{\star} = 10^{-4}$. We utilize the recursive equations outlined in Section III-A for various distributions $\Lambda(x)$, both regular and irregular. The value of $G^{\star}$ is depicted in Fig. 2 as a function of $\bar{N}_{\text{AP}}$. Firstly, we observe that, as $\eta \to 0$ (i.e., $\bar{N}_{\text{AP}} \to 1$), $G^{\star}$ converges to the load threshold over the collision channel in the cell-based setting, as reviewed in Section II. This is due to the fact that, for $\eta \to 0$, the few APs generated by the PPP are scattered far away from each other, causing users to perceive only one AP: in this scenario, we revert to the cell-based architecture. Secondly, we note that repeating more times seems to degrade $G^{\star}$, for $\bar{N}_{\text{AP}}$ sufficiently larger than one. This phenomenon, peculiar of cell-free architectures, results in the optimal distributions observed in cell-based architectures becoming sub-optimal in distributed environments. This occurs as packets are repeated, leveraging both the spatial and temporal dimensions. The effective repetition distribution $\Gamma(x)$, therefore, deviates significantly from $\Lambda(x)$, hindering a straightforward reuse of the optimal distributions derived, e.g., in [8].

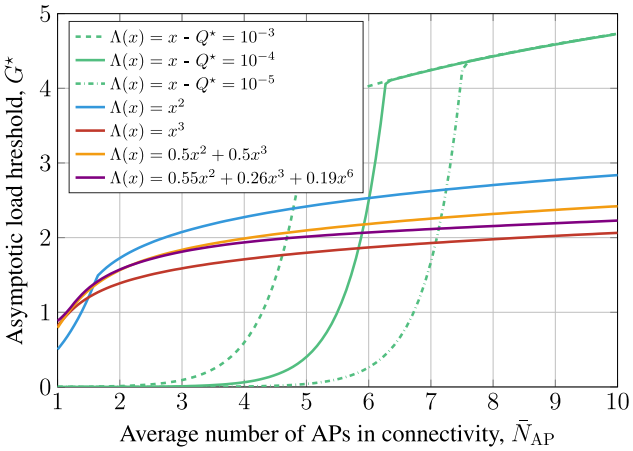

Fig. 2. Dependency between asymptotic traffic threshold and the average number of access points in connectivity of an active user in a cell-free scenario.

Special attention is warranted for the scheme with a single packet transmission, i.e., $\Lambda(x) = x$. This scheme, performing poorly in a cell-based scenario, can exploit the AP density to spatially repeat packets in a cell-free architecture, achieving favorable threshold values. The analysis reveals that for a sufficiently large AP density, it can outperform other distributions. However, the range of $\bar{N}_{\text{AP}}$ values for which $\Lambda(x) = x$ yields good results is highly dependent on the target $Q^{\star}$. Indeed, a phase transition behavior is evident in the figure, as detailed in Section III-B. As $\bar{N}_{\text{AP}}$ progressively increases, we initially observe an exponential trend, as expressed by (11). However, at a certain value of $\bar{N}_{\text{AP}}$, a marked shift in trend occurs, leading to a transition in the achievable load, now characterized by (13). A similar phase transition can be observed for $\Lambda(x) = x^2$, with the first exponential behavior $G^{\star} = e^B/2$ predicted in Section III-B.

B. Simulation

To illustrate the accuracy of the proposed load threshold analysis, we use a simulator to evaluate the PLR metric. In particular, the generation of APs and users occurs in a square with a side length equal to $20R$, where the disk model radius is $R = 100$ m, value that could represent an equivalent cell-based scenario adopting picocells. To mitigate edge effects, we adopt a wrapped geometry. Specifically, we envelop a square area around the edges to simulate a network with infinite area [17]. Moreover, when shadowing is considered, we set $\sigma_{\text{dB}} = 10 \log_{10}(\exp(2\sigma)) = 6$ and $\alpha = 3.67$. The threshold $\bar{P}_{\text{th}}$ is computed according to (6) to have the same effective area $|\mathcal{A}|$ of the disk model. This ensures that the density evolution threshold is valid for both disk and shadowing-based models. The frame length is set to $N_s = 50$ slots.

In Fig. 3 and in Fig. 4, we report the results for: the simulations with and without shadowing; the corresponding asymptotic thresholds derived in Section III-A; and the lower bounds derived in Section III-C for the scheme without shadowing. In particular, we show results imposing $\bar{N}_{\text{AP}} = 5$ and $\bar{N}_{\text{AP}} = 15$. Firstly, we emphasize that the lower bounds accurately estimate the error floor regions of the performance curves under disk model assumptions, while the density evolution analysis successfully predicts the locations of the waterfall

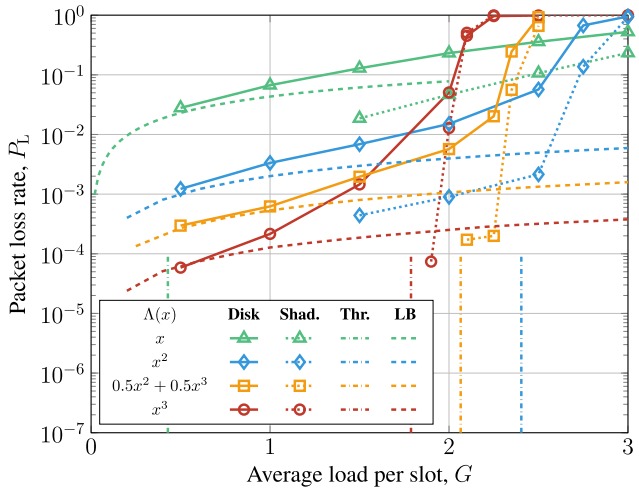

Fig. 3. Performance analysis of CRA schemes against the average traffic per slot fixing $\bar{N}_{\mathrm{AP}} = 5$. Curves with marker: simulation.

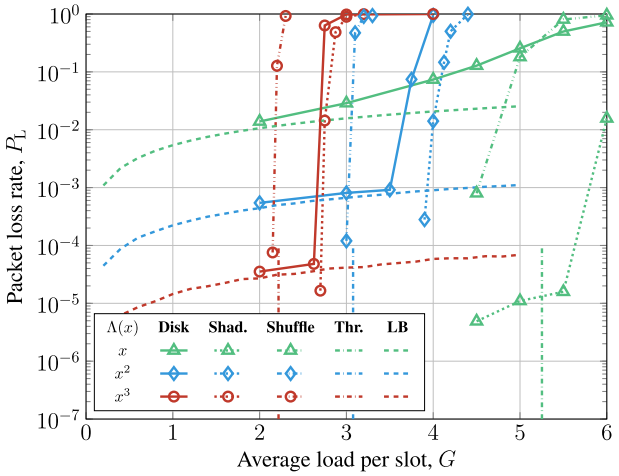

Fig. 4. Performance analysis of CRA schemes against the average traffic per slot fixing $\bar{N}_{\mathrm{AP}} = 15$. Curves with marker: simulation.

regions. Secondly, we observe a slight discrepancy between the density evolution analysis and the simulation curves. This gap can be attributed to the fact that density evolution does not account for spatial correlations between users and APs. In reality, users transmit replicas only to nearby APs, creating an effect during SIC akin to spatial coupling [18], [19]. To substantiate this claim, we conduct a simulation where, after users and APs generation, we shuffle their adjacency matrix to break this correlation. The results, reported in Fig. 4, perfectly align with the density evolution analysis. Thirdly, we observe the beneficial effect arising from uncorrelated shadowing. This is because the unresolvable collision discussed in Section III-C could become resolvable in the presence of shadowing. The probability that two users transmitting in the same slots are seen by the same APs is lower in this context, resulting in PLRs smaller than the disk model lower bound. Finally, it is worth stressing that the ALOHA case $\Lambda(x) = x$, typically ineffective in cell-based scenarios, could play a crucial role in the SIC-enhanced cell-free architecture for interconnecting low-power devices, depending on the reliability target.

V. Conclusion

The growing interest in cell-free architectures and grant-free protocols for next-generation wireless networks necessitates reliable design tools to optimize and compare various solutions. In pursuit of this goal, we introduce a novel density evolution-based tool designed for both a disk model connectivity and one in the presence of shadowing. Key findings from our analysis suggest that adopting low repetition degrees is advisable when AP density is high.

References

[1] H. Q. Ngo, A. Ashikhmin, H. Yang, E. G. Larsson, and T. L. Marzetta, "Cell-free massive MIMO versus small cells," *IEEE Trans. Wireless Commun.*, vol. 16, no. 3, pp. 1834–1850, Mar. 2017.

[2] Ö. T. Demir, E. Björnson, and L. Sanguinetti, "Foundations of user-centric cell-free massive MIMO," *Found. Trends Signal Process.*, vol. 14, nos. 3–4, pp. 162–472, 2021.

[3] H. ElSawy, A. Sultan-Salem, M.-S. Alouini, and M. Z. Win, "Modeling and analysis of cellular networks using stochastic geometry: A tutorial," *IEEE Commun. Surveys Tuts.*, vol. 19, no. 1, pp. 167–203, 1st Quart., 2017.

[4] Z. Chen and E. Björnson, "Channel hardening and favorable propagation in cell-free massive MIMO with stochastic geometry," *IEEE Trans. Commun.*, vol. 66, no. 11, pp. 5205–5219, Nov. 2018.

[5] A. Papazafeiropoulos, P. Kourtessis, M. Di Renzo, S. Chatzinotas, and J. M. Senior, "Performance analysis of cell-free massive MIMO systems: A stochastic geometry approach," *IEEE Trans. Veh. Technol.*, vol. 69, no. 4, pp. 3523–3537, Apr. 2020.

[6] P. Parida and H. S. Dhillon, "Cell-free massive MIMO with finite fronthaul capacity: A stochastic geometry perspective," *IEEE Trans. Wireless Commun.*, vol. 22, no. 3, pp. 1555–1572, Mar. 2023.

[7] M. Ibrahim, S. Elhoushy, and W. Hamouda, "Uplink performance of mmWave-fronthaul cell-free massive MIMO systems," *IEEE Trans. Veh. Technol.*, vol. 71, no. 2, pp. 1536–1548, Feb. 2022.

[8] G. Liva, "Graph-based analysis and optimization of contention resolution diversity slotted Aloha," *IEEE Trans. Commun.*, vol. 59, no. 2, pp. 477–487, Feb. 2011.

[9] T. J. Richardson, M. A. Shokrollahi, and R. L. Urbanke, "Design of capacity-approaching irregular low-density parity-check codes," *IEEE Trans. Inf. Theory*, vol. 47, no. 2, pp. 619–637, Feb. 2001.

[10] E. Paolini, G. Liva, and M. Chiani, "Coded slotted ALOHA: A graph-based method for uncoordinated multiple access," *IEEE Trans. Inf. Theory*, vol. 61, no. 12, pp. 6815–6832, Dec. 2015.

[11] J. Su, G. Ren, and B. Zhao, "NOMA-based coded slotted ALOHA for machine-type communications," *IEEE Commun. Lett.*, vol. 25, no. 7, pp. 2435–2439, Jul. 2021.

[12] L. Valentini, M. Chiani, and E. Paolini, "A joint PHY and MAC layer design for coded random access with massive MIMO," in *Proc. IEEE Global Commun. Conf.*, Dec. 2022, pp. 2505–2510.

[13] J. Haghighat and T. M. Duman, "An energy-efficient feedback-aided irregular repetition slotted Aloha scheme and its asymptotic performance analysis," *IEEE Trans. Wireless Commun.*, vol. 22, no. 12, pp. 9808–9820, Dec. 2023.

[14] K.-H. Ngo, G. Durisi, and A. G. I. Amat, "Age of information in prioritized random access," in *Proc. 55th Asilomar Conf. Signals, Syst., Comput.*, Oct. 2021, pp. 1–19.

[15] J. F. C. Kingman, *Poisson Processes*. Hoboken, NJ, USA: Wiley, 1993.

[16] L. Valentini, A. Giorgetti, and M. Chiani, "Density estimation in randomly distributed wireless networks," *IEEE Trans. Wireless Commun.*, vol. 21, no. 8, pp. 6687–6697, Feb. 2022.

[17] U. K. Ganesan, E. Björnson, and E. G. Larsson, "An algorithm for grant-free random access in cell-free massive MIMO," in *Proc. IEEE 21st Int. Workshop Signal Process. Adv. Wireless Commun. (SPAWC)*, May 2020, pp. 1–5.

[18] G. Liva, E. Paolini, M. Lentmaier, and M. Chiani, "Spatially-coupled random access on graphs," in *Proc. IEEE Int. Symp. Inf. Theory*, Jul. 2012, pp. 478–482.

[19] L. Valentini, M. Chiani, and E. Paolini, "Massive grant-free access with massive MIMO and spatially coupled replicas," *IEEE Trans. Commun.*, vol. 70, no. 11, pp. 7337–7350, Nov. 2022.

Open Access funding provided by 'Alma Mater Studiorum - Università di Bologna' within the CRUI CARE Agreement